Transportmetrica A: Transport Science
Publication details, including instructions for authors and subscription information:
http://www.tandfonline.com/loi/ttra21

Microscopic traffic behaviour modelling and simulation for lane-blocking arterial incidents

Jiuh-Biing Sheu [a]

[a] Institute of Traffic and Transportation, National Chiao Tung University , 4F, 114 Chung Hsiao W. Rd., Sec. 1, Taipei , Taiwan

Published online: 23 May 2011.

To cite this article: Jiuh-Biing Sheu (2013) Microscopic traffic behaviour modelling and simulation for lane-blocking arterial incidents, Transportmetrica A: Transport Science, 9:4, 335-357, DOI: 10.1080/18128602.2011.577042

To link to this article: http://dx.doi.org/10.1080/18128602.2011.577042

Transportmetrica A: Transport Science, 2013
Vol. 9, No. 4, 335–357, http://dx.doi.org/10.1080/18128602.2011.577042

Taylor & Francis
Taylor & Francis Group

Microscopic traffic behaviour modelling and simulation for lane-blocking arterial incidents

Jiuh-Biing Sheu*

Institute of Traffic and Transportation, National Chiao Tung University, 4F, 114 Chung Hsiao W. Rd., Sec. 1, Taipei, Taiwan

(*Received 10 March 2010; final version received 29 March 2011*)

Incident-induced driver behaviour modelling is essential to analyse non-recurrent traffic congestion problems. However, such research is inadequate in such areas as traffic flow prediction, traffic simulation and incident management. This article presents microscopic lane traffic models to characterise incident-induced driver behaviour including car following and lane changing conducted under conditions of lane-blocking arterial incidents. To demonstrate the validity of the proposed models, a specific microscopic traffic simulation program embedded with the proposed incident-induced lane traffic behaviour models is tested by comparing simulation data with video-based incident data collected from five incident events. Preliminary test results indicate that the proposed microscopic traffic behaviour models permit not only reproducing incident-induced traffic behaviour but also characterising incident effects on lane traffic phenomena.

Keywords: incident-induced traffic modelling; lane changing; microscopic traffic simulation

1. Introduction

Modelling incident-induced lane traffic manoeuvres remains challenging in the field of traffic flow theory and related areas such as traffic simulation and incident management (Hawas 2007). In reality, numerous related issues including queue overflows and gridlocks caused by lane-blocking incidents have resulted in difficulty in the operations of traffic control and management (Sheu 2003, Qi *et al*. 2009). Compared with incident-free cases, lane-blocking incidents may result in anomalous increases in lane changes upstream from incident sites, thus creating unusual queue lengths and delays (Sheu and Ritchie 2001). From a psychological point of view, drivers' rubbernecking and driving with pressure while passing by an incident site also add complexity and uncertainty to incident traffic characterisation and prediction (Holland 1998, Hamdar and Mahmassani 2008). Second, lane changes can generate other traffic flow phenomena, such as secondary accidents and spillback events, during an incident as lane changes from blocked lanes can cause irregular traffic interference among adjacent lanes that adversely affect road safety. Thus, modelling incident-induced lane traffic manoeuvres is vital to develop sophisticated traffic flow theories, as well as advanced traffic control and management methodologies, that address non-recurrent traffic congestion problems.

*Email: jbsheu@mail.nctu.edu.tw

Microscopic traffic behaviour modelling has garnered increased recognition for its ability to accurately reproduce incident-induced lane traffic dynamics, particularly lane-changing behaviour during incident-induced lane traffic jams (Chowdhury *et al*. 2000). In contrast with the aforementioned macroscopic methodology, which assumes that traffic has fluid-like dynamics, microscopic methodology treats incident-induced traffic flow as a nonequilibrium system of particles with transitional jamming phases caused by unusual speed and lane-changing variations. Janowsky and Lebowitz (1992) applied the asymmetrical simple exclusion process that uses a unique transition probability to characterise incident-induced traffic jams on a one-dimensional lattice. Nagatani (1994) extended this asymmetrical simple exclusion model for two-lane highway incident cases. Kurata and Nagatani (2003) employed an optimal velocity model to generate a two-lane traffic model in which symmetrical lane-changing rules were adopted to investigate incident-induced traffic congestion. Kerner and Klenov (2003) and Kerner *et al*. (2006) proposed parameter-rich microscopic models to investigate spatial-temporal traffic congestion patterns of highway bottlenecks, and discussed the effects of lane changes on the structure of highway bottlenecks and moving traffic jams. This was followed by the development of a cellular automation (CA)-based traffic model by Zhu *et al*. (2009), in which the symmetrical and asymmetrical lane-changing rules proposed by Chowdhury *et al*. (1997) were utilised to improve the model's ability to characterise incident-affected lane changing. Additionally, some studies which did not focus on incident cases have proposed sophisticated microscopic models that rationalise the entire driver decision process associated with lane changing (Choudhury 2005, Ramanujam 2007, Toledo *et al*. 2007, 2009, Webster *et al*. 2008).

Despite the advances made by these pioneering scholars in microscopic traffic modelling, incident-induced driver behaviour modelling on urban streets remains challenging. The intricacies in modelling are based on the discontinuity of traffic flows caused by traffic signal control, accompanied by the network effect of traffic flows moving across blocks characterised by various geometric characteristics. For instance, vehicles in blocked lanes must change lanes. However, changing lanes at will in this instance is often difficult due to various traffic conditions such as arriving and discharging vehicles in adjacent lanes. When an incident is located on a short block or at an intersection, a bottleneck and serious network-wide gridlock likely occur, increasing the complexity in reproducing traffic flows on urban streets. Moreover, unlike freeway incidents with a one-dimensional impact on traffic flows, the impact of urban street incidents can be two-dimensional (network-wide) and irregularly change with time when neighbouring traffic signal controls are not coordinated (Sheu 2002).

Accordingly, this work applies a microscopic traffic behaviour modelling approach that characterises incident-induced intra-lane and inter-lane traffic manoeuvres. This study primarily focuses on cases of arterial lane blocking (i.e. incidents on a roadway between two adjacent intersections). The proposed models are applicable to multi-lane blocking as well as single-lane blocking.

The remainder of this article is organised as follows. Section 2 introduces the proposed lane traffic behaviour models to elucidate the rationale of using the proposed models to characterise incident-induced intra-lane and inter-lane traffic manoeuvres. Section 3 presents the primary procedures and analytical results for model tests to verify whether the proposed models permit accurately characterising incident-induced lane traffic phenomena on arterials. Finally, Section 4 gives concluding remarks and directions for future research.

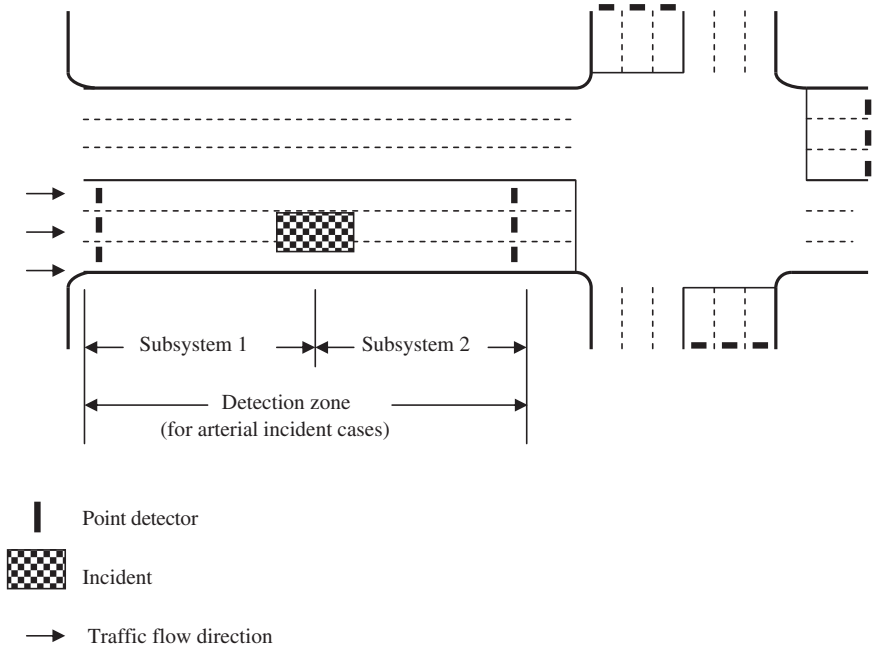

Figure 1. Definition of a detection zone.

2. Traffic behaviour modelling

The proposed microscopic lane traffic behaviour models contain two components: intra-lane and inter-lane traffic behaviour models to characterise incident-induced lane traffic manoeuvres present in the area upstream of an incident site on an arterial, namely, subsystem 1 of a detection zone (Figure 1). According to analytical results and simple identification logic, the microscopic intra-lane and inter-lane traffic manoeuvres were classified into several types to model the movement of an individual vehicle within subsystem 1 (Figure 2). This work aims at modelling incident-induced car-following and lane-changing manoeuvres conducted in blocked lanes upstream from an incident site, which are described in the following subsections.

2.1. *Intra-lane traffic behaviour modelling*

In this subsection, we first introduce three types of inter-vehicle dynamic spacing to facilitate intra-lane traffic behaviour characterisation, followed by the modelling of specific intra-lane traffic behaviour present in these three dynamic spacing scenarios.

2.1.1. *Inter-vehicle dynamic spacing*

In adopting the concept of dynamic thresholds of inter-vehicle spacing proposed by Sheu (2007), this work specified three inter-vehicle dynamic spacing types: (1) free-flow movement; (2) incident-induced car following and (3) mandatory braking. These three

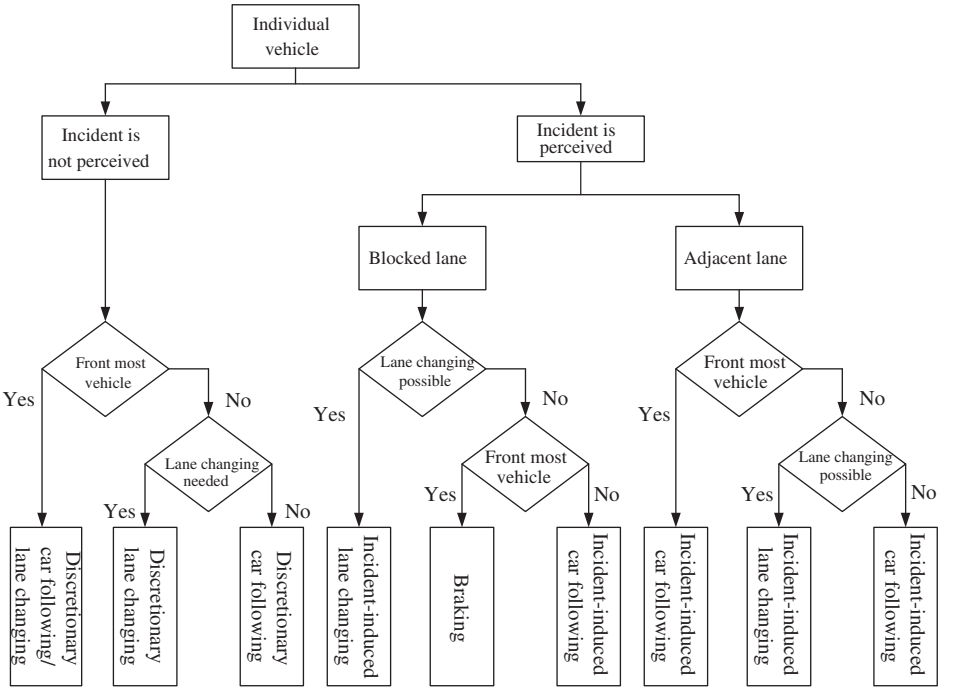

Figure 2. Classification of lane traffic manoeuvres in subsystem 1.

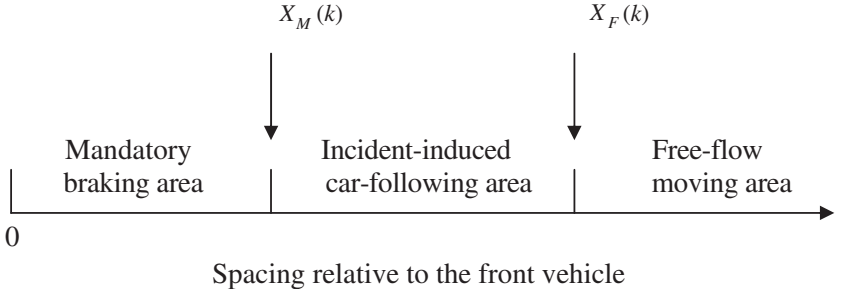

Figure 3. Illustration of the dynamic spacing for intra-lane traffic modelling.

spacing types are defined to characterise three types of driver behaviour of a given vehicle moving in a blocked lane of subsystem 1. Figure 3 shows the three types of inter-vehicle spacing, and the corresponding dynamic boundaries, i.e. $X_M(k)$ and $X_F(k)$, which indicate the required spacing for mandatory braking (M) and free-flow movement (F) at a given time step k. Vehicles upstream from an incident site must brake when the dynamic inter-vehicle spacing is $<X_M(k)$. Conversely, when the spacing exceeds $X_F(k)$, free-flow lane manoeuvres are allowed; otherwise, vehicles may change lanes to pass the incident site. The following gives the derivational procedures for these dynamic thresholds, followed by the description of the proposed models.

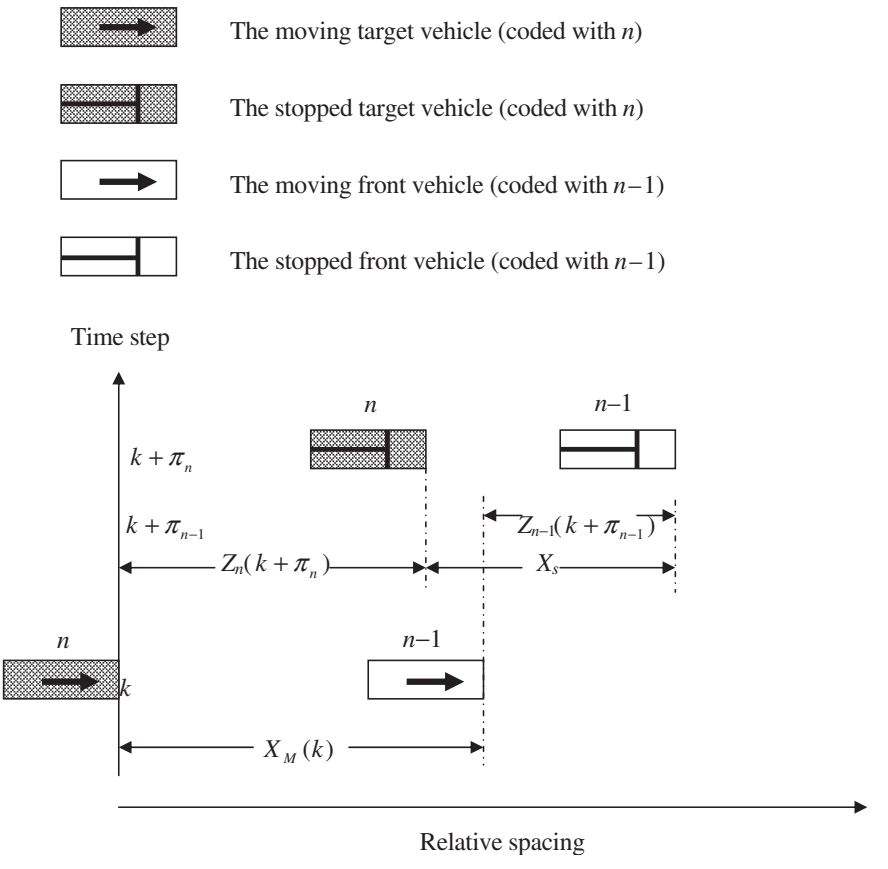

Figure 4. Illustration of the critical spacing for mandatory braking.

The derivation of $X_M(k)$ is based primarily on dynamic safety spacing that must be maintained between a target and the vehicle in front when both drivers brake (Figure 4). Such braking may exist under the condition that both the target and front vehicles are approaching vehicles queued upstream from the incident site. In considering the mandatory braking that may be conducted by a front vehicle at any given time step k, the target vehicle must maintain the minimum safety spacing to ensure safe stopping. Accordingly, this work derives $X_M(k)$ as follows:

$$X_M(k) = X_s + Z_n(k+\pi_n) - Z_{n-1}(k+\pi_{n-1}) \tag{1}$$

$$\Rightarrow X_M(k) = X_s + \left\{ V_n(k) \times \tau_n - \frac{[V_n(k)]^2}{2D_n} \right\} + \frac{[V_{n-1}(k)]^2}{2D_{n-1}} \tag{2}$$

where X_s (unit: m) is the minimum safety spacing between the target and front vehicles, and is to be calibrated in the section of model tests; $Z_n(k+\pi_n)$ and $Z_{n-1}(k+\pi_{n-1})$ are the braking distances (unit: m) associated with target vehicle n and front vehicle $n-1$ that are

fully stopped at time steps $k+\pi_n$ and $k+\pi_{n-1}$, respectively; $V_n(k)$ and $V_{n-1}(k)$ are the speeds (unit: m/s) of target vehicle n and front vehicle $n-1$ at time step k, respectively; D_n and D_{n-1} represent maximum deceleration rates (m/s^2) of target vehicle n and front vehicle $n-1$, respectively, and both depend on the type of vehicle and τ_n is the reaction time (unit: s) associated with target vehicle n, which is calibrated in the section of model tests.

This work now considers the following interesting cases to determine the validity of the aforementioned derivation. For simplification, we assume parameters D_n and D_{n-1} depending only on vehicle type. Thus, if the target vehicle and front vehicle are the same vehicle type ($D_n = D_{n-1}$), then Equation (2) can be rewritten as

$$X_M(k) = X_s + \left\{ V_n(k) \times \tau_n - \frac{[V_n(k)]^2 - [V_{n-1}(k)]^2}{2D_n} \right\} \tag{3}$$

Equation (3) characterises the relative speed relationship between the target and front vehicles, and the corresponding effect on the determination of $X_M(k)$. Given the instantaneous speed of the front vehicle (i.e. $V_{n-1}(k)$), as the speed of the target vehicle increases, the value of $X_M(k)$ increases, implying that the target vehicle needs a longer braking distance when it runs at a higher speed relative to low speed conditions. Conversely, when the driver of the target vehicle perceives that the speed of the front vehicle has increased (i.e. $V_n(k) < V_{n-1}(k)$), the value of $X_M(k)$ may decline. Notably, in applications such as microscopic simulation, Equation (3) can be integrated with specific stochastic processes that represent various driver characteristics to determine the specific value of $X_M(k)$ for any given vehicle.

In contrast with $X_M(k)$, $X_F(k)$ is derived based on the assumption that target vehicle movement is independent of any behaviour of the front vehicle in a free-flow area. This work now considers a specific case, in which the target vehicle can accelerate without considering the front vehicle braking at time step k. Therefore, the generalised form of $X_F(k)$ should theoretically satisfy the following condition:

$$X_F(k) \geq X_M(k) + \frac{[V_n(k+1)]^2 - [V_n(k)]^2}{2a_n(k)} - \frac{[V_{n-1}(k)]^2}{2d_{n-1}(k)} \tag{4}$$

where $V_n(k+1)$ (unit: m/s) is the speed of target vehicle n at time step k+1; $a_n(k)$ is the acceleration (unit: m/s^2) of target vehicle n at time step k and $d_{n-1}(k)$ is the instantaneous deceleration (unit: m/s^2) by front vehicle $n-1$ at time step k.

Similarly, the following critical condition is used to determine the lower bound of $X_F(k)$ ($\tilde{X}_F(k)$). According to the aforementioned assumption for $X_F(k)$, any given target vehicle n moving in a free-flow area should be allowed to undertake maximum acceleration even when the front vehicle undertakes maximum deceleration. Thus, the lower bound of $X_F(k)$ ($\tilde{X}_F(k)$) is

$$\tilde{X}_F(k) = X_M(k) + \left[V_n(k) + \frac{A_n}{2} \right] - \frac{[V_{n-1}(k)]^2}{2D_{n-1}} \tag{5}$$

where A_n is maximum acceleration (unit: m/s^2) of target vehicle n.

Based on the specifications of the three dynamic spacing types bounded by $X_M(k)$ and $X_F(k)$, intra-lane traffic manoeuvres that potentially occur in these three dynamic spacing scenarios are modelled, and described as follows.

2.1.2. *Scenario 1 – mandatory braking*

This scenario models the mandatory braking behaviour of any vehicle under the condition that it cannot change lanes at a given time step. According to the boundaries of $X_M(k)$ in Equation (2), any target vehicle may be forced to brake at the current time step k once the relative spacing ($X_{n,n-1}(k)$) between target vehicle n and front vehicle $(n-1)$ is $\leq X_M(k)$. Thus, the following condition (Equation (6)) must be satisfied:

$$X_{n,n-1}(k) \leq X_s + \left\{ V_n(k) \times \tau_n - \frac{[V_n(k)]^2}{2D_n} \right\} + \frac{[V_{n-1}(k)]^2}{2D_{n-1}} \tag{6}$$

The instantaneous deceleration ($d_n(k+\tau_n)$) by target vehicle n at time step $k+\tau_n$ can then be derived as

$$d_n(k+\tau_n) = \frac{[V_n(k)]^2}{2\left\{ X_s + V_n(k) \times \tau_n + \frac{[V_{n-1}(k)]^2}{2D_{n-1}} - X_{n,n-1}(k) \right\}} \tag{7}$$

Notably, the aforementioned mandatory braking occurs most frequently under the condition that the target vehicle in a blocked lane is approaching either an incident site or a stopped vehicle (i.e. $V_{n-1}(k) = 0$). In such a case, Equation (7) can be further simplified as

$$d_n(k+\tau_n) = \frac{[V_n(k)]^2}{2\left[X_s + V_n(k) \times \tau_n - X_{n,n-1}(k) \right]} \tag{8}$$

Furthermore, consider a special case in which reaction time τ_n is too small. Under this condition, the formulation of deceleration in response to stalled vehicles in the mandatory braking area can be expressed as

$$d_n(k) = \frac{[V_n(k)]^2}{2\left[X_s - X_{n,n-1}(k) \right]} \tag{9}$$

Notably, the aforementioned case may be acceptable for automatic highway systems (AHSs) because the effect of such human factors as reaction time on traffic manoeuvres may be insignificant.

2.1.3. *Scenario 2 – incident-induced car-following*

This scenario describes procedure for deriving the proposed incident-induced car-following model, which characterises the speed adjustment of any target vehicle moving within the incident-induced car-following area bounded by $X_M(k)$ and $X_F(k)$. The proposed incident-induced car-following model is constructed based on the fundamentals of collision avoidance (CA) models[1] (Gipps 1981, Benekohal and Treiterer 1989, Brokua *et al.* 1991, McDonald *et al.* 1994, Kumamoto *et al.* 1995, Brackstone and McDonald 1999). However, compared with existing CA models, the target vehicle in the proposed model adjusts its speed based on the front vehicle and front platoon, which are further ahead and approaching the incident site. Arguments supporting this idea can also be found in the literature of multi-anticipative car-following which hinges on the manoeuvres of perceived more than one vehicles moving ahead (Bexelius 1968, Lenz *et al.* 1999,

Hoogendoorn and Ossen 2006, Hoogendoorn *et al*. 2009). Note that the proposed model considers the phenomenon in that, under incident conditions, any target vehicle can adjust to incident effects on traffic flows, and thus, tailor its speed based on a safe distance from the vehicle in front and the perceived aggregate speed of the traffic platoon upstream of the incident site in a blocked lane. Particularly, the corresponding effect of the front platoon may increase as the target vehicle approaches the incident site. The incident-induced car-following model is proposed as Equation (10).

$$E_n(k+\tau_n) = \left[1-\omega\left(X_{n,p}(k),k\right)\right]\times\alpha_1\left\{\left[X_{n,I}(k)-X_{n-1,I}(k)\right]-S_{n,n-1}(k)\right\}+\omega\left(X_{n,p}(k),k\right) \times\alpha_2\left[\frac{\sum_{i=1}^{N_p(k)}V_i(k)}{N_p(k)}-V_n(k)\right] \tag{10}$$

where $E_n(k+\tau_n)$ (unit: m/s^2) is the incident-induced speed adjustment by target vehicle n at time step $k+\tau_n$; $N_p(k)$ is the number of vehicles in the platoon upstream from the incident site in the blocked lane at time step k; $X_{n,I}(k)$ (unit: m) is the geographical spacing between target vehicle n and incident I observed at time step k; $X_{n-1,I}(k)$ (unit: m) is the spacing between front vehicle $n-1$ and incident I; $S_{n,n-1}(k)$ (unit: m) is the dynamic safety space between target vehicle n and front vehicle $n-1$ at time step k that is acceptable to target vehicle n; α_1 and α_2 are two pre-set parameters (units: s^{-2} and s^{-1}); and $\omega(X_{n,p}(k),\ k)$ is a weighting value indicating the relative magnitude of the effect of platoon p on the speed adjustment of target vehicle n compared with the effect caused by front vehicle $n-1$. In this work, we assume $\omega\left(X_{n,p}(k),\ k\right)$ is a negative exponential function with respect to $X_{n,I}(k)$, and is given by

$$\omega\left(X_{n,p}(k),\ k\right) = e^{-bX_{nI}(k)} \tag{11}$$

where b is a positive parameter (unit, m^{-1}). Equation (11) represents a weighting value indicating the relative influence of the perceived platoon p on the speed adjustment of target vehicle n compared with the influence from the front vehicle $n-1$. Herein, $\omega(X_{n,p}(k),\ k)$ is formulated based on the following postulation from a psychological point of view. When approaching incident site I, the closer target vehicle n is to I, its speed adjustment relies on platoon p in the blocked lane more than on front vehicle $n-1$ due to the target driver's curiosity about incident situations, termed incident-induced rubbernecking effect in Sheu (2008). At the current model developmental stage, $\omega(X_{n,p}(k),\ k)$ is assumed to be a negative exponential function for simplicity. It is noted that $\omega(X_{n,p}(k),\ k)$ should not be limited to a negative exponential function. Instead, it can also be formulated in other forms (e.g. linear functions) to appropriately characterise the aforementioned relationship between the target vehicle's speed adjustment and perceived platoon relative to the front vehicle. Additionally, $S_{n,n-1}(k)$ is regarded as the dynamic length (unit: m) of the front vehicle $n-1$ perceived by target vehicle n (Chou and Sheu 1992), and thus $S_{n,n-1}(k)$ is denoted by

$$S_{n,n-1}(k) = L_{n-1} + V_n(k)\times\tau_n \tag{12}$$

where L_{n-1} represents the physical length (unit: m) of front vehicle $n-1$.

The following case discusses two interesting cases to which the proposed incident-induced car-following model is applied.

- Case 1: Perception of platoon queuing at an incident site

This case illustrates the situation in which the target driver perceives the queuing platoon near an incident site, which may lead to $\frac{\sum_{i=1}^{N_p(k)} V_i(k)}{N_p(k)} = 0$. Under this condition, the speed adjustment estimation in Eqation (10) becomes

$$E_n(k+\tau_n) = \left[1-\omega\left(X_{n,p}(k),k\right)\right] \times \alpha_1 \times \left[X_{n,I}(k) - X_{n-1,I}(k) - L_{n-1}\right] - \left\{\alpha_1 \times \tau_n \times \left[1-\omega\left(X_{n,p}(k),k\right)\right] + \alpha_2 \times \omega\left(X_{n,I}(k),k\right)\right\} \times V_n(k) \quad (13)$$

where $E_n(k+\tau_n)$ can be either positive or negative, depending on the difference (i.e. $X_{n,I}(k) - X_{n-1,I}(k) - L_{n-1}$) in the geographic spacing between the target and front vehicles, as well as the instantaneous speed ($V_n(k)$) of target vehicle n.

- Case 2: No front vehicle perceived

Further, consider a special case in which the target vehicle perceives no front vehicle as it approaches the incident site. Correspondingly, $X_{n,I}(k) - X_{n-1,I}(k) - L_{n-1}$, which is on the right-hand side of Equation (13), is zero. Thus, $E_n(k+\tau_n)$ is negative, and can be denoted by

$$E_n(k+\tau_n) = -\left\{\alpha_1 \times \tau_n \times \left[1-\omega\left(X_{n,p}(k),k\right)\right] + \alpha_2 \times \omega\left(X_{n,p}(k),k\right)\right\} \times V_n(k) \quad (14)$$

That is, target vehicle n typically decelerates, the absolute value of which is proportional to the running speed when approaching an incident site. Notably, the generalisations in this scenario also apply to the case in which no platoon exists at the incident site.

Additionally, the meaning of the upper and lower bounds of the weight value $\omega(X_{n,p}(k),\ k)$ is also worth discussing. When $\omega(X_{n,p}(k),\ k)$=0, the target vehicle's speed adjustment depends on front vehicle $n-1$, and thus, may lead to an estimation result similar to that estimated by existing CA models. Conversely, when $\omega(X_{n,p}(k),\ k)$=1, target vehicle n is closest to the study site, and the same result as that in Equation (14) can be derived. This condition also applies to the case in which the target vehicle and front vehicle are considered members of the same platoon when approaching the incident site. A related application example worth noting is that in which the target vehicle is linked with other vehicles, including the front vehicle in the AHS operating environment, in response to a lane-blocking incident occurring ahead. In other cases, various human factors can be considered to rationalise the $\omega(X_{n,p}(k),\ k)$ function.

2.1.4. *Scenario 3 – free-flow moving*

The proposed traffic behaviour model in this scenario is mainly used to estimate the speed adjustment of target vehicle n, which is in free-flow area under the condition $X_{n,I}(k) - X_{n-1,I}(k) \geq \tilde{X}_F(k)$. Under this condition, the speed adjustment by the target vehicle at time step $k+\tau$ ($F_n(k+\tau)$) is estimated by

$$F_n(k+\tau_n) = \beta \times \left[\hat{V}_n - V_n(k)\right] \quad (15)$$

where $\hat{V}_n$ is the free-flow speed (unit: m/s) of target vehicle n under the current traffic condition and β is a pre-determined parameter (unit: s^{-1}).

2.2. *Inter-lane traffic behaviour modelling*

This subsection models mandatory lane-changing manoeuvres of vehicles present upstream from an incident site using a two-stage modelling approach. According to Sheu and Ritchie (2001), lane-changing manoeuvres within a defined detection zone (Figure 1) can be classified as mandatory lane changing in subsystem 1, and discretionary lane changing in subsystem 2. Compared with conventional lane-changing models, the primary feature of the proposed model is that mandatory lane-changing behaviour of any vehicle in subsystem 1 is completed via two stages – pre-action judgement and in-action lane changing. These two stages are described as follows.

2.2.1. *Stage 1: pre-action judgement*

The decision-making model in this stage determines whether mandatory lane changing is needed during the subsequent time steps. The logic rules developed here are based on concepts of driving psychology and psychophysical theory. This work adopts the ideas from quantum mechanics-based optical flow models (Baker 1999, Sheu 2008) that utilise psychophysical momentum to quantify the stimulus-response behaviour of a driver. Therefore, the proposed model considers the following two psychological factors: (1) perceived lane-changing status in the target lane (i.e. the lane the target vehicle is in) and (2) the relative platoon speeds in adjacent lanes compared with that in the target lane.

The determination of perceived lane-changing status relies on the comparison of frequencies of lane changing from the target lane to adjacent lanes (termed lane-changing-out) and from adjacent lanes to the target lane (termed lane-changing-in) within the visual scope of a target driver. Figure 5 shows the visual scope q specified for target vehicle n in recognising the lane-changing status in the target lane, where $X_n^q(k)$ is the longitudinal boundary of visual scope (Figure 5), and is denoted by

$$X_n^q(k) = \frac{2w \times \left[X_{n,I}(k) - X_{n-1,I}(k) - L_{n-1}\right]}{W_{n-1}} \tag{16}$$

where w is lane width (unit: m), and W_{n-1} is the physical width (unit: m) of front vehicle $n-1$. This study infers that the driver of the target vehicle (termed target driver in the following text) is prone to change lanes when the perceived lane-changing-out frequency is greater than lane-changing-in frequency within the visual scope over a given period.

Notably, mandatory lane changing can be conducted anywhere in subsystem 1, and $X_n^q(k)$ is time-dependent. Therefore, the corresponding values of $X_n^q(k)$ in different dynamic spacing cases are worth discussing.

- Case 1: Moving in the mandatory braking area

Although changing lanes in the mandatory braking area is difficult, aggressive drivers exist. In this case, Equation (6) is applied to remove the safety spacing, X_s, from Equation (6), yielding

$$X_n^q(k) = \frac{2w \times \left\{V_n(k) \times \tau_n - \frac{[V_n(k+\tau_n)]^2}{2D_n} + \frac{[V_{n-1}(k)]^2}{2D_{n-1}} - L_{n-1}\right\}}{W_{n-1}} \tag{17}$$

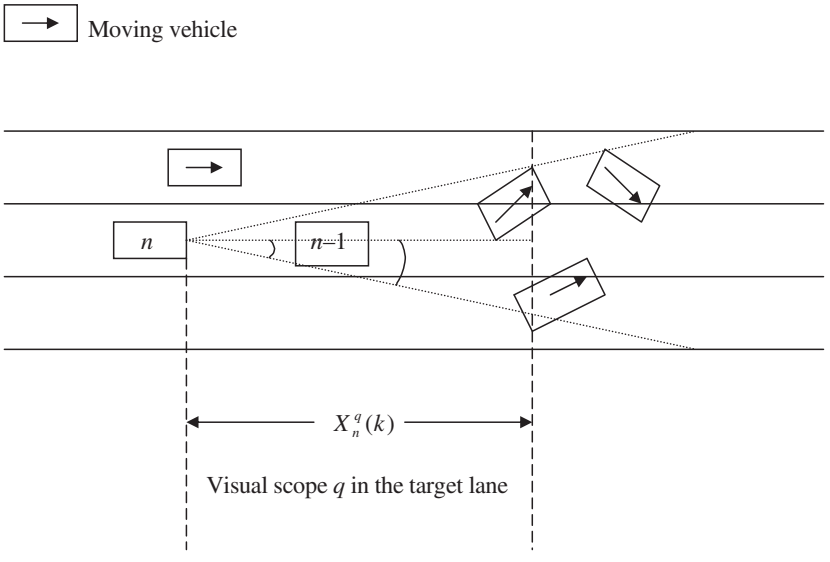

Figure 5. Visual scope for judging the lane-changing status in the target lane.

Similarly, one noteworthy case is that in which the target vehicle is the only vehicle in front of an incident in the blocked lane in subsystem 1. Under this condition, the inter-lane behaviour of target vehicle n is directly processed by the model constructed in the second-stage once incident I is within visual boundary $X_{n,I}^q(k)$ which is given by

$$X_{n,I}^q(k) = \frac{2w \times \left\{ V_n(k) \times \tau_n - \frac{[V_n(k)]^2}{2D_n} - L_I \right\}}{W_{n-1}} \tag{18}$$

where L_I is longitudinal distance (unit: m) of incident site I.

- Case 2: Movement in the incident-induced car-following area

In this case, the dynamic spacing between target vehicle n and front vehicle $n-1$ is estimated using Equation (5); this value is then input into Equation (16) to obtain the corresponding value of $X_n^q(k)$ (Equation (19)) for the case of vehicles moving in the incident-induced car-following area

$$X_n^q(k) = \frac{2w \times \left\{ \left[V_n(k) + \frac{A_n}{2} \right] - \frac{[V_{n-1}(k)]^2}{2D_{n-1}} - L_{n-1} \right\}}{W_{n-1}} \tag{19}$$

- Case 3: Movement in the free-flow area

Note that in Case 2, the lower bound of $X_F(k)$ (i.e. $\tilde{X}_F(k)$ in Equation (5)), is used. Thus, Equation (19) can be rewritten as Equation (20) to determine the corresponding value of $X_n^q(k)$ for the case of a target vehicle moving in the free-flow area.

$$X_n^q(k) > \frac{2w \times \left\{ \left[V_n(k) + \frac{A_n}{2} \right] - \frac{[V_{n-1}(k)]^2}{2D_{n-1}} - L_{n-1} \right\}}{W_{n-1}} \tag{20}$$

In reality, Equation (20) implies that any target vehicle in the free-flow area may remain in the same lane for the following two reasons. First, as mentioned, any target vehicle in the free-flow area can move at will in any lane. Therefore, the target vehicle does not need to make a lane change decision before entering the incident-induced car-following area. Second, the estimate of $X_n^q(k)$ in Equation (20) may be outside the normal range of a driver's visibility, particularly when a vehicle is travelling at high speeds. Thus, we assume that the lane-changing status in front of the front vehicle is difficult to observe when the target vehicle is moving in the free-flow area.

In addition to perceived lane-changing status in the target lane, the relative platoon speed in an adjacent lane is also a significant factor when determining lane-changing behaviour. By utilising $X_n^q(k)$, the target vehicle may compare the relative aggregate platoon speed in the target lane with that in any lane directly adjacent to the target lane. Once platoon speed in the adjacent lane is perceived as higher than that in the target lane, the target vehicle may change lanes in subsequent time steps. Conversely, given the lane-changing-out frequency is greater than the lane-changing-in frequency in the target lane for a prolonged period, this phenomenon may reduce the speeds of vehicles moving in adjacent lanes as lane densities are increasing. Under this situation, the willingness of the target driver to change lanes may decrease, despite the perceived high lane-changing-out frequency, which may, according to the proposed model, cause driver to change lanes. Furthermore, the lane-changing-out frequency may not remain high continuously as adjacent lane densities increase. Briefly, a trade-off exists between the effects of perceived lane-changing status in the target lane and the relative platoon speeds in adjacent lanes. Accordingly, the corresponding logic rules are developed to determine whether or not the target driver considers change lanes in the next time step.

Clearly, given that an incident is known to all drivers, the first stage of pre-action decision-making can be omitted, and the model constructed in the second stage can be applied directly to process the lane changing action of any given target vehicle in subsystem 1.

2.2.2. *Stage 2: in-action lane-changing operation*

This scenario investigates the factors influencing lane-changing manoeuvres, given that the target driver feels the necessity of conducting lane changing which is determined in the previous stage. Compared to the previous decision, the decision made at this stage helps the driver change lanes safely and smoothly in response to varied traffic conditions in adjacent lanes and blocked lanes. For this purpose, this work proposes four required constraints – two constraints for intra-lane traffic factors, and the other two constraints for inter-lane traffic factors. They are then used to determine whether incident-induced mandatory lane changing can be completed successfully at the next time step by the target vehicle. That is, mandatory lane changing can be implemented only when these four conditions are satisfied during the current time step. The details of the derivations of these constraints are as follows.

- Constraint 1: Restricted target vehicle turning angle n ($\theta_n(k)$)

This constraint accounts for potential conflict points that may exist between the target and front vehicles in the target lane when the target vehicle changes lanes (Figure 6).

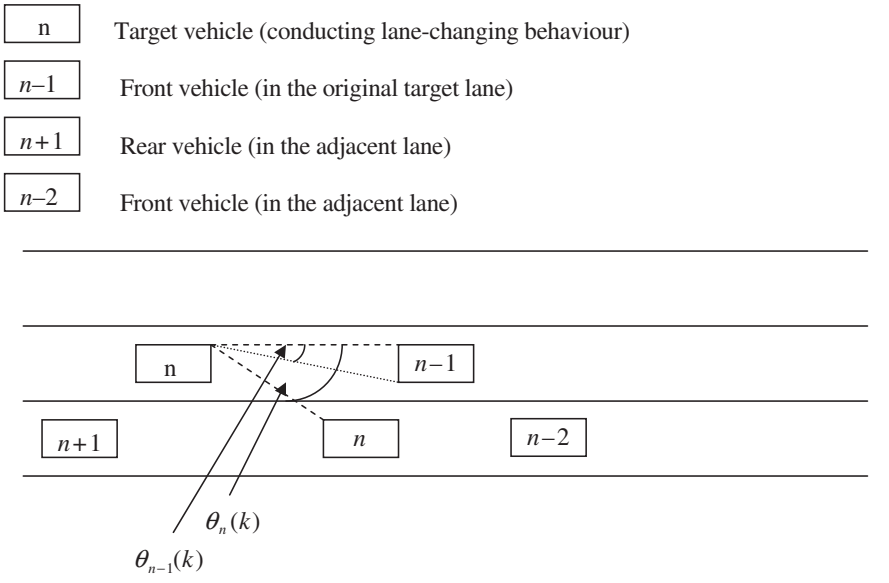

Figure 6. Illustration of the turning angle restriction.

To change lanes, the condition of $\theta_n(k) \geq \theta_{n-1}(k)$ must be satisfied, where $\theta_{n-1}(k)$ is given by

$$\theta_{n-1}(k) = \tan^{-1}\left\{\frac{W_{n-1}(k)}{X_{n,I}(k) - X_{n-1,I}(k) - L_{n-1} - X_s}\right\} \tag{21}$$

- Constraint 2: Restricted latitudinal spacing between the target and front vehicles in the original target lane

Given $\theta_n(k)$, the following condition must hold to avoid a collision between the target vehicle and front vehicle in the original target lane during lane changing.

$$\Phi_n^{\sin(\theta_n)}(k+t) \geq WD_{n-1}(k+t) \tag{22}$$

where $\Phi_n^{\sin(\theta_n)}(k+t)$ is the moving distance (unit: m) of target vehicle n in the latitudinal direction in while changing lanes at time step $k+t$; $WD_{n-1}(k+t)$ is the dynamic width (unit: m) of front vehicle $n-1$ in the original target lane at time step $k+t$ and t is to the amount of time spent by target vehicle n moving at a maximum safe distance in the longitudinal direction while changing lanes to avoid a collision with front vehicle $n-1$ in the original target lane. Notably, the concept of $WD_{n-1}(k+t)$, which is similar to the dynamic vehicular length described previously, is utilised to determine the latitudinal safe space between target vehicle n and front vehicle $n-1$ in the original target lane during lane changing. Theoretically, $\Phi_n^{\sin(\theta_n)}(k+t)$, $WD_{n-1}(k+t)$ and t are functions of microscopic

characteristics of the target and front vehicles in the original target lane, and can be derived as:

$$\Phi_n^{\sin\theta_n}(k+t)=\frac{\left\{\begin{array}{c}3\left[\vec{V}_n^{\cos}(k)\right]^2+8a_n^{\ln}(k)s(k)-2\left[\vec{V}_n^{\cos}(k)\right]\times\sqrt{4\left[\vec{V}_n^{\cos}(k)\right]^2+8a_n^{\ln}(k)s(k)}\\+2\left[\vec{V}_n^{\sin}(k)\right]\times\left\{\sqrt{4\left[\vec{V}_n^{\cos}(k)\right]^2+8a_n^{\ln}(k)s(k)}-\left[\vec{V}_n^{\cos}(k)\right]\right\}\end{array}\right\}}{2a_n^{\ln}(k)} \tag{23}$$

$$WD_{n-1}(k+t)=W_{n-1}\times[1+\alpha_3\times V_{n-1}(k)] \tag{24}$$

$$t=\frac{\sqrt{4\left[\vec{V}_n^{\cos}(k)\right]^2+8a_n^{\ln}(k)s(k)}-2\vec{V}_n^{\cos}(k)}{2a_n^{\ln}(k)} \tag{25}$$

where $a_n^{\ln}(k)$ is the acceleration/deceleration (unit: m/s^2) of the target vehicle at time step k in while changing lanes; α_3 is a pre-set parameter (unit: s/m); $\vec{V}_n^{\cos}(k)$ is the relative speed (unit: m/s) of target vehicle n compared with that of front vehicle $n-1$ in the longitudinal direction at time step k, and, similarly, $\vec{V}_n^{\sin}(k)$ is that in the latitudinal direction; $s(k)$ is the relative moving distance (unit: m) allowed for target vehicle n in the longitudinal direction while changing lanes to avoid a collision with the front vehicle in the original target lane at time step k. Herein, $\vec{V}_n^{\cos}(k)$, $\vec{V}_n^{\sin}(k)$ and $s(k)$ can be further expressed as Equations (26), (27) and (28), respectively.

$$\vec{V}_n^{\cos}(k)=V_n(k)\times\cos[\theta_n(k)]-V_{n-1}(k) \tag{26}$$

$$\vec{V}_n^{\sin}(k)=V_n(k)\times\sin[\theta_n(k)] \tag{27}$$

$$s(k)=X_{n,I}(k)-X_{n-1,I}(k)-L_{n-1}-X_s \tag{28}$$

Notably, we assume the speed of front vehicle $n-1$ is constant when target vehicle n changes lanes. Thus, the lane-changing manoeuvres of the target vehicle in response to the changing speed of the front vehicle warrant further investigation.

- Constraint 3: Restriction of the dynamic safety space between target vehicle n and rear vehicle $n+1$ in the adjacent lane into which the target vehicle will move

This constraint applies a minimum safety spacing between target vehicle n and rear vehicle $n+1$ in the adjacent lane when the target vehicle moves into the adjacent lane. In this scenario, this work applies a novel derived conflict point ($X_c(k+t)$) to formulate the constraint rather than employing the concept of $X_F(k)$ directly, which was constructed previously in addressing issues associated with intra-lane traffic manoeuvres. That is, the proposed intra-lane models may not be applicable at the moment of lane changing. Under such a transitional condition where the front target vehicle is moving from the original target lane to an adjacent lane, the rear vehicle in the adjacent lane cannot respond safely

to the traffic manoeuvre of the target vehicle within an extremely short time interval. Thus, $X_c(k+t)$ is given by

$$X_c(k+t) = X_{n,I}(k) - s(k) \tag{29}$$

which corresponds to the instantaneous distance between target vehicle n and rear vehicle $n+1$ in the longitudinal direction in the adjacent lane.

Utilising the notation of $X_c(k+t)$ defined previously, the following condition must be satisfied to consider the dynamic safety spacing ($X_{n+1,X_C}(k+t)$) between the conflict point $X_c(k+t)$ and rear vehicle $n+1$ in the adjacent lane when target vehicle n changes lanes at time step k.

$$X_{n+1,X_C}(k+t) - X_s \geq V_{n+1}(k+t) \times \tau_n - \frac{[V_{n+1}(k+t+\tau_n)]^2}{2D_{n+1}} + \frac{[V_n(k+t)]^2}{2D_n} \tag{30}$$

where $V_n(k+t)$ and $V_{n+1}(k+t)$ are the speeds (unit: m/s) of target vehicle n and rear vehicle $n+1$ at time step $k+t$, respectively; similarly, $V_{n+1}(k+t)$ is the speed (unit: m/s) of rear vehicle $n+1$ at time step $k+t+\tau_n$; D_{n+1} is the predetermined maximum deceleration (unit: m/s^2) of rear vehicle $n+1$.

- Constraint 4: Restricted dynamic safety spacing between target vehicle n and the new front vehicle $n-2$ in the adjacent lane, into which the target vehicle will move

This constraint deals with the constraint of the dynamic safety spacing ($X_{X_C,n-2}(k+t)$) between target vehicle n and front vehicle $n-2$ in the adjacent lane when the target vehicle changes lanes at time step k. Similar to Constraint 3, the following condition must be satisfied to ensure that the mandatory lane-changing manoeuvre of the target vehicle is allowed at time step k:

$$X_{X_C,n-2}(k+t) - X_s \geq V_n(k+t) \times \tau_n - \frac{[V_n(k+t+\tau_n)]^2}{2D_n} + \frac{[V_{n-2}(k+t)]^2}{2D_{n-2}} \tag{31}$$

In Equation (31), $V_n(k+t+\tau_n)$ is the speed (unit: m/s) of target vehicle n at time step $k+t+\tau$; and similarly, $V_{n-2}(k+t)$ and D_{n-2} are the speed (unit: m/s) and preset maximum deceleration (unit: m/s^2) of the front vehicle in the adjacent lane at time step $k+t$, respectively.

3. Model tests

This section describes the procedures for testing the ability of the proposed microscopic traffic behaviour models to accurately characterise incident-induced lane traffic phenomena on arterials. The technique utilised for performance evaluation is a microscopic traffic simulation program developed for this work. The proposed incident-induced lane traffic behaviour models are integrated into the developed traffic simulation program. Evaluation measurements were based mainly on a comparison of simulation data generated by the traffic simulation program and video-based real incident data collected with the assistance of the Traffic Engineering Office (TEO) of Taipei City Government, Taiwan.

The database used in model tests was primarily generated by processing the video-based data collected from five respective traffic incidents occurring at five arterials located at the city of Taipei, as indicated in Figure 7. Therein, one camera installed at an

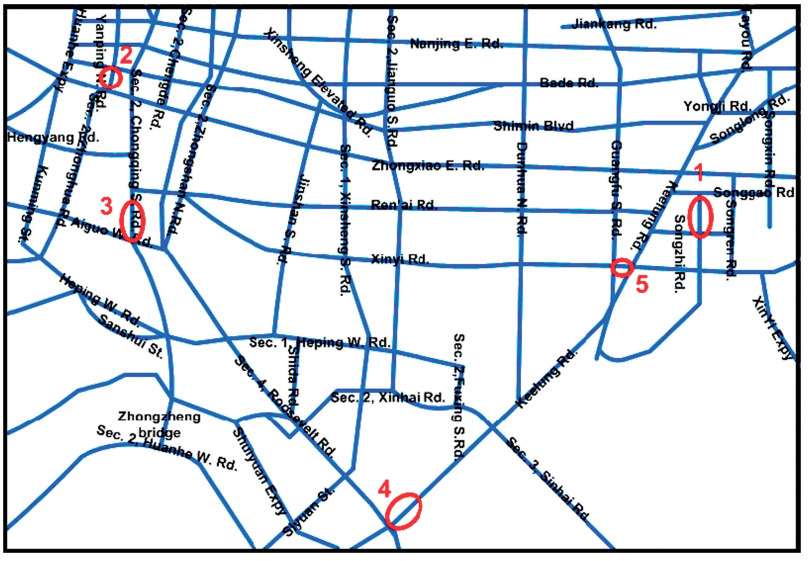

Figure 7. Locations of studied incident cases.

intersection near each studied location was used to monitor real-time local traffic situations. The studied incident cases were videotaped by these cameras. Among these five sampled incident events, one is a low-volume incident case (Case 1), two are medium-volume incidents (Cases 2 and 3) and two are high-volume incidents (Case 4 and 5). The geometric and traffic characteristics observed in the study cases are summarised in Table 1.

The data acquisition procedure in this study involves two scenarios: (1) input data processing for simulation and (2) output data generated for calibration and validation. We used videotapes provided by TEO of Taipei City Government to generate the incident database. Observed from the videotapes, we generated 30 s lane-based data including the arrival rates, arrival speeds and traffic composition associated with those links where incidents were located (termed incident links) for the use as input data of simulation. Additionally, we collected several traffic measurements, including vehicle-based incident-induced link travel time, lane usage and lane-changing fractions (for each 30 seconds), for model evaluation.

To test the proposed incident-induced lane traffic behaviour models, a microscopic traffic simulation program was developed in Turbo C computer language. Model calibration was conducted in advance of model tests in this study. The data used in mode calibration was a part of the collected video-based data. Therein, one half of the collected video-based data was used for model calibration and the rest for model tests. Table 2 lists the primary parameters set for simulation. Based on Abdulhai *et al.* (1999, 2002), this work primarily calibrated the parameters of minimum safety spacing (X_s) and mean reaction time (τ) associated with each type of vehicle as these parameters determine driver decisions during car-following and lane-changing behaviour in microscopic traffic simulation. To seek for appropriate values for X_s and τ, this work adopted a two-dimensional search process (Abdulhai *et al.* 1999) which permits minimising the discrepancy between the

Table 1. Geometric and traffic characteristics of studied incident sites.

Characteristics / Incident case	Number of lanes in arterial (ln)	Block length (m)	Hourly volume (veh/h/ln)	Incident location	Incident duration (min)
Case 1 (low-volume)	3	101	453	Upstream, outside lane	27
Case 2 (medium-volume)	4	208	980	Midstream, inside lane	42
Case 3 (medium-volume)	3	592	864	Upstream, central lane	28
Case 4 (high-volume)	4	290	1124	Downstream, central lane	34
Case 5 (high-volume)	4	187	1277	Downstream, outside lane	39

Table 2. Preset vehicle characteristics and calibrated traffic parameters.

Vehicle characteristics				Calibrated traffic parameters			
Vehicle type		Length L_* (m)	Width W_* (m)	Maximum acceleration A_* (m/s^2)	Maximum deceleration D_* (m/s^2)	Minimum safety spacing X_s (m)	Mean reaction time τ(s)
Light vehicle	Car	4.0	3.56	3.56	7.30	5.2	0.88
	Light goods vehicle	6.0	2.22	2.22	7.30	7.2	0.97
Heavy vehicle	Truck	11.0	1.4	1.4	5.63	13.6	1.25
	Bus	10.0	1.4	1.4	5.63	12.6	1.25
Other key parameter			α_1 (s^{-2})	α_2 (s^{-1})	β (s^{-1})	b (m^{-1})	
Calibrated value			0.22	0.13	0.31	0.06	

simulation output and field observations, but requires numerous simulation runs for every point in the search space. As the search domain was unknown, we used our own empirical iterative search process that searches in one direction only at a time. For example, given X_s is fixed at its best known value obtained from the previous search iterations, one-directional search is performed for the other parameter, say τ, within reasonable upper and lower bounds. Once the optimal τ value is found, it gets fixed and its range is empirically reduced around this value, followed by the next-round search for X_s. Such an iterative search process continues until improvements diminish. The primary steps of the calibration procedure can also be found in Abdulhai et al. (1999), and omitted in this work for our space concern. In terms of maximum acceleration (A_*) and deceleration (D_*), this work referred to Pline (1999), and then determined these two parameters while considering emergency braking, which is common in incident cases. Such vehicular characteristics as physical length and width of different vehicles were pre-determined.

The model tests in this work aim to verify the performance of the proposed lane traffic behaviour models for arterial incident cases and to determine the advantages of these models for use in simulating incident-induced traffic manoeuvres. Thus, this work compared simulation data generated by the proposed incident-induced traffic simulation program with video-based real incident data.

The following five traffic measurements were utilised: (1) traffic arrivals, (2) average arrival speeds, (3) incident-induced lane-changing fractions, (4) link travel time and (5) lane usage on the incident-affected link. Therein, simulation data used to test traffic arrivals, average arrival speed, and lane-changing fractions were collected at 30 s intervals, whereas link travel time was measured on a vehicle-by-vehicle basis during incidents. Herein, lane usage was measured by a lane-specific traffic density divided by the associate link traffic density observed during an incident. Accordingly, it seems agreeable that lane usage has a close relationship with either lane-specific flows or time-based lane occupancies, and thus is also suitable for indicating the distribution of lane-specific traffic loads revealed in an incident link. Traffic arrivals and arrival speeds were used to test the acceptability of simulated traffic flow conditions upstream of the incident site. The measurements of lane-changing fractions were used to assess the validity of the proposed lane-changing logic under lane-blocking incident conditions. Conversely, measurements of link travel time and lane usage were utilised to assess the performance of the proposed models in characterising incident effects on macroscopic traffic states.

This study examined simulated traffic arrivals, average arrival speed, and lane-changing fractions using mean absolute percentage errors (MAPEs). In this test scenario, the 30 s simulation data samples were generated using the proposed simulation program, and then compared with video-based data via the MAPE statistics. All simulated values were aggregated measurements from 10 simulations for each incident case. To demonstrate the relative advantage of the proposed model used in characterising incident-induced traffic behaviour, the MAPE statistics yielded from the simulation program without incident-induced lane traffic behaviour models were also generated for comparison. Table 3 summarises test results for traffic arrivals, average arrival speeds and lane-changing fractions.

The test results of Table 3 indicate that, overall, the simulated values of lane traffic variables such as traffic arrivals, arrival speeds and lane-changing fractions reproduced by the proposed models fit video-based data better than those without incident-induced behaviour models. Although there are no general guidelines for when an MAPE value is sufficiently high, it is commonly agreed that forecast output should not be accepted when a value of MAPE $>50\%$. Moreover, several classes are suggested in Lewis (1982) for the assessment using MAPE values, where 0.2–0.5 is regarded as a reasonable range for accepting MAPE statistics, and relatively $\leq 10\%$ is a demanding threshold for MAPE values. Conversely, some MAPE values yielded in the case without incident-induced traffic behaviour models exceed the loose threshold 0.5, indicating the necessity of incorporating the proposed models into the reproduction of incident-induced lane traffic manoeuvres.

Furthermore, the MAPE values obtained under medium-volume incident conditions (i.e. Cases 2 and 3) are, overall, higher than those obtained in low-volume and high-volume incident cases. Therein, we found that unlike low- and high-volume incident cases in which the lane traffic flow conditions change stably, the lane traffic variables (particularly traffic arrivals and lane-changing fractions) observed in Cases 2 and 3 are likely to vary irregularly with time. Such a feature of significant traffic randomness existing in the medium-volume incident cases can be the major reason for resulting in higher MAPE values in the study.

Conversely, test results for lane usage and averaged link travel time and lane usage (Table 4) indicate the performance of the proposed models in dealing with lane traffic manoeuvres as vehicles move through the link on which the incident occurred. Overall, the

Table 3. Test results (I).

Incident case \ MAPE measurement	Traffic arrivals	Arrival speed	Lane-changing fractions
Case 1 (low-volume)	0.15 (0.18)	0.19 (0.37)	0.23 (0.44)
Case 2 (medium-volume)	0.43 (0.53)	0.38 (0.66)	0.47 (0.83)
Case 3 (medium-volume)	0.32 (0.44)	0.25 (0.59)	0.39 (0.72)
Case 4 (high-volume)	0.26 (0.41)	0.21 (0.44)	0.31 (0.63)
Case 5 (high-volume)	0.22 (0.38)	0.28 (0.48)	0.30 (0.58)
Overall performance	0.28 (0.39)	0.26 (0.51)	0.34 (0.64)
Test result (compared with threshold: 0.5)	Accepted	Accepted	Accepted

Note: MAPE values yielded without incident-induced traffic behaviour models in parentheses.

Table 4. Test results (II).

		Lane usage (%)			
Incident case	Measurement data source	Inside lane	Central lane(s)	Outside lane	Averaged link travel time (s)
Case 1 (low-volume)	Videotape	33.7	42.7	23.6	43.4
	Model	36.3	38.6	25.1	41.7
	Relative error (%)	7.7	−9.6	6.4	−3.9
Case 2 (medium-volume)	Videotape	14.2	46.9	38.9	65.5
	Model	11.7	47.5	40.8	70.2
	Relative error (%)	−17.6	1.3	4.9	7.2
Case 3 (medium-volume)	Videotape	36.1	25.2	38.7	69.8
	Model	39.6	23.5	36.9	75.4
	Relative error (%)	9.7	−6.7	−4.7	8.0
Case 4 (high-volume)	Videotape	41.6	11.9	46.5	78.3
	Model	42.8	12.4	43.8	83.2
	Relative error (%)	2.8	4.2	−5.8	6.3
Case 5 (high-volume)	Videotape	38.9	51.4	9.7	86.6
	Model	42.3	49.3	8.4	82.7
	Relative error (%)	8.7	−4.1	−13.4	−4.5

absolute values of the resulting relative errors are lower than 0.2, and 90% of them are lower than 0.1, i.e. satisfactory. That is, the proposed models can estimate average link travel time for arterial incident cases by appropriately reproducing incident-induced driver behaviour. Such a generalisation, on the other hand, implies that the effects of incidents on intra-lane and inter-lane traffic manoeuvres can be addressed utilising the proposed microscopic lane traffic behaviour models. Furthermore, the ability of the proposed models to reproduce lane usage of the incident site is also satisfactory. According to test results, the proposed models permit reproducing incident-induced mandatory lane changes from blocked lanes to adjacent lanes upstream of the incident site, as well as discretionary lane changes once vehicles pass the incident. Thus, simulated measurements of lane usage obtained by the proposed models generally match real values.

4. Conclusions and recommendations

This study modelled inter-lane and intra-lane traffic manoeuvres under arterial lane-blocking incidents and simulated incident-induced lane traffic behaviour using a microscopic traffic modelling approach. This work also analysed the effects of lane-blocking incidents on lane traffic behaviour, including lane-changing and car-following behaviours. Novel microscopic traffic behaviour models were formulated to characterise incident-induced lane traffic manoeuvres, followed by the development of a microscopic simulation program to demonstrate the applications of the proposed models. In analysing microscopic incident-induced lane manoeuvres, this work specified three types of dynamic spacing for free-flow moving traffic, incident-induced car following and mandatory braking, respectively. The intra-lane traffic manoeuvres and related factors were then characterised and formulated. Additionally, a two-stage lane-changing mechanism, which has two levels of functionality – (1) pre-action decision-making and (2) in-action lane-changing operation, was proposed to reproduce mandatory lane-changing behaviour of any given vehicle moving in blocked lanes upstream of an incident site.

Preliminary test results indicate that the proposed microscopic lane traffic behaviour models can characterise incident-induced lane traffic behaviour and incident effects on inter-lane and intra-lane traffic manoeuvres. Analytical results of model tests under different traffic flow conditions have also demonstrated the potential effect of traffic randomness on the proposed models' overall performance particularly under medium-volume traffic flow conditions. Therein, we found that lane traffic states such as traffic arrivals and lane-changing fractions under medium-volume incident conditions are likely vary irregularly with time, not as stably as those observed in low- and high-volume incident cases. This finding may also imply that specific coordinated traffic signal controls are needed at two successive intersections that cover an incident site to regulate traffic arrivals upstream of the incident site, particularly for arterial incidents with medium volumes. Furthermore, there is still room for model improvement and tests with more demanding thresholds (e.g. MAPE values $\leq$10%) although the MAPE test results are overall acceptable in this study. The heterogeneity of driver reaction time can be another issue. As the proposed models are microscopic, and formulated in a personal decision domain, a more appropriate measure is to treat driver reaction time as a random variable following a constrained distribution bounded by lower and upper bounds.

The proposed models are currently being extended to intersection incident cases in which incident-induced lane traffic manoeuvres may be relatively more complicated due to the effects of signal controls. Further testing the proposed models using relatively more real data for incident cases is needed. Moreover, applications of the proposed lane traffic models also warrant further research. The applications suggested include uses of the proposed models in developing a network-based microscopic traffic simulator, and exploring the effects of human factors (e.g. awareness and driving pressure) on microscopic traffic manoeuvres, such as queuing and changing lanes, for various lane-blocking incidents. Comparison or integration of related macroscopic and microscopic models with the proposed models also warrants additional research. For example, some early studies (e.g. Hidas 2002, 2005, Chevallier and Leclercq 2009) are outstanding in dealing with the response of a following vehicle to, and interaction with, the subject vehicle changing lanes based on the concept of gap acceptance. Further research comparing existing models with the proposed models may advance incident-induced

lane-changing modelling. Additionally, the effect of the perceived vehicular platoons in adjacent lanes on the target vehicle's speed adjustment also needs further investigation to improve the proposed incident-induced car-following model. Most importantly, we hope that this study can stimulate research devoted to the development of microscopic incident-related traffic simulators.

Acknowledgements

This research was supported by grant NSC 99-2410-H-009-031-MY3 from the National Science Council of Taiwan. The author also wishes to thank the referees for their helpful comments. Any errors or omissions remain the sole responsibility of the authors.

Note

1. The idea common to existing CA models is that by manipulating the basic Newtonian equations, a safe car-following spacing is determined to avoid a collision, given that the front vehicle acts unpredictably.

References

Abdulhai, B., Sheu, J.-B., and Recker, W. 1999. Simulation of ITS on the Irvine FOT area using "Paramics 1.5" scalable microscopic traffic simulator: phase I: model calibration and validation. California PATH Research Report, UCB-ITS-PRR-99-12.

Abdulhai, B., Sheu, J.-B., and Recker, W., 2002. Development and performance evaluation of an ITS-ready microscopic traffic model for Irvine, California. *Journal of Intelligent Transportation Systems*, 7 (1), 79–102.

Baker, R.G.V., 1999. On the quantum mechanics of optic flow and its application to driving in uncertain environments. *Transportation Research Part F*, 2, 27–53.

Benekohal, R.F. and Treiterer, J., 1989. CARSIM: car following model for simulation of traffic in normal and stop and go conditions. *Transportation Research Record*, 1194, 99–111.

Bexelius, S., 1968. An extended model for car-following. *Transportation Research*, 2 (1), 13–21.

Brackstone, M. and McDonald, M., 1999. Car-following: a historical review. *Transportation Research Part F*, 2, 181–196.

Brokua, F., *et al*., 1991. Cooperative driving: basic concepts and a first assessment of intelligent cruise control strategies. *Proceedings of the DRIVE conference*, 908–929. Amsterdam: Elsevier.

Chevallier, E. and Leclercq, L., 2009. Do microscopic merging models reproduce the observed priority sharing ratio in congestion. *Transportation Research Part C*, 17, 328–336.

Choudhury, C.F., 2005. Modeling lane-changing behavior in presence of exclusive lanes. Ph.D. Thesis, Massachusetts Institute of Technology.

Chou, Y.-H. and Sheu, J.-B., 1992. A simulation model of mixed traffic flow in roundabouts. *Transportation Planning Journal*, 21 (3), 301–333.

Chowdhury, D., Wolf, D.E., and Schreckenberg, M., 1997. Particle hopping models for two-lane traffic with two kinds of vehicles: effects of lane-changing rules. *Physica A*, 235 (3–4), 417–439.

Chowdhury, D., Santen, L., and Schadschneider, A., 2000. Statistical physics of vehicular traffic and some related systems. *Physics Reports*, 329, 199–329.

Gipps, P.G., 1981. A behavioural car following model for computer simulation. *Transportation Research B*, 15, 105–111.

Hamdar, S.H. and Mahmassani, H.S., 2008. From existing accident-free car-following models to colliding vehicles. *Transportation Research Record*, 2088, 45–56.

Hawas, Y.E., 2007. A microscopic simulation model for incident modeling in urban networks. *Transport Planning and Technology*, 30, 289–309.
Hidas, P., 2002. Modelling lane changing and merging in microscopic traffic simulation. *Transportation Research Part C*, 10, 351–371.
Hidas, P., 2005. Modelling vehicle interactions in microscopic simulation of merging and weaving. *Transportation Research Part C*, 13, 37–62.
Holland, E.N., 1998. A generalized stability criterion for motorway traffic. *Transportation Research B*, 32 (2), 141–154.
Hoogendoorn, S.P. and Ossen, S., 2006. Empirical analysis of two-leader car-following behavior. *European Journal of Transport and Infrastructure Research*, 6 (3), 229–246.
Hoogendoorn, S.P., Ossen, S., and Schreuder, M., 2009. Empirics of Multianticipative car-following behavior. Presented at the Transportation Research Board Annual Meeting 2009, January 11–15, Washington, DC.
Janowsky, S.A. and Lebowitz, J.L., 1992. Finite-size effects and shock fluctuations in the asymmetric simple-exclusion process. *Physical Review A*, 45 (2), 618–625.
Kerner, B.S. and Klenov, S., 2003. Microscopic theory of spatial-temporal congested traffic patterns at highway bottlenecks. *Physical Review E*, 68, 036130.
Kerner, B.S., *et al*., 2006. Microscopic features of moving jams. *Physical Review E*, 73, 046107.
Kumamoto, H., *et al*., 1995. Rule based cognitive animation simulator for current lane and lane change drivers. Proceedings of the Second World Congress on ATT, 1746–1752. Yokohama, Japan, November 1995.
Kurata, S. and Nagatani, T., 2003. Spatio-temporal dynamics of jams in two-lane traffic with a blockage. *Physica A*, 318 (3–4), 537–550.
Lenz, H., Wagner, C.K., and Sollacher, R., 1999. Multi-anticipative car-following model. *The European Physical Journal B*, 7, 331–335.
Lewis, C.D., 1982. Industrial and business forecasting methods: a practical guide to exponential smoothing and curve fitting, Presented at Butterworth Scientific, Boston, MA.
McDonald, M., Brackstone, M., and Jeffery, D. 1994. Simulation of lane usage characteristics on 3 lane motorways. *Proceedings of the 27th ISATA Conference*, Aachen Germany, November 1994.
Nagatani, T., 1994. Dynamic jamming transition induced by a car accident in traffic-flow model of a two-lane roadway. *Physica A*, 202 (3–4), 449–458.
Pline, J.L., ed., 1999. *Traffic engineering handbook*, 5th ed. Institute of Transportation Engineers. Washington, DC.
Qi, Y., Teng, H., and Martinelli, D.R., 2009. An investigation of incident frequency, duration and lanes blockage for determining traffic delay. *Journal of Advanced Transportation*, 43, 275–299.
Ramanujam, V., 2007. Lane changing models for arterial traffic. Ph.D. Thesis, Massachusetts Institute of Technology.
Sheu, J.-B. and Ritchie, S.G., 2001. Stochastic modeling and real-time prediction of vehicular lane-changing behavior. *Transportation Research-Part B*, 35 (7), 695–716.
Sheu, J.-B., 2002. A stochastic optimal control approach to real-time incident-responsive traffic signal control at isolated intersections. *Transportation Science*, 36 (4), 418–434.
Sheu, J.-B., 2003. A stochastic modeling approach to real-time prediction of queue overflows. *Transportation Science*, 37 (1), 97–119.
Sheu, J.-B., 2007. Microscopic modeling and control logic for incident-responsive automatic vehicle movements in single-automated-lane highway systems. *European Journal of Operational Research*, 182, 640–662.
Sheu, J.-B., 2008. A quantum mechanics-based approach to model incident-induced dynamic driver maneuvers. *Physica D*, 137, 1800–1814.
Toledo, T., Koutsopoulos, H.N., and Ben-Akiva, M., 2007. Integrated driving behavior modeling. *Transportation Research Part C*, 15, 96–112.

Toledo, T., Koutsopoulos, H.N., and Ben-Akiva, M., 2009. Estimation of an integrated driving behavior model. *Transportation Research Part C*, 17, 365–380.

Webster, N.A., Suzuki, T., and Kuwahara, M., 2008. Tactical lane change model with sequential maneuver planning. *Transportmetrica*, 4, 63–78.

Zhu, H.B., Lei, L., and Dai, S.Q., 2009. Two-lane traffic simulations with blockage induced by an accident car. *Physica A*, 388, 2903–2910.